SLAC-PUB-6479
April 20, 1994
T/E/AS

Electroweak Baryogenesis and Standard Model CP Violation

Patrick Huet and Eric Sather*
Stanford Linear Accelerator Center
Stanford University
Stanford, California 94309

Abstract

We analyze the mechanism of electroweak baryogenesis proposed by Farrar and Shaposhnikov in which the phase of the CKM mixing matrix is the only source of CP violation. This mechanism is based on a phase separation of baryons via the scattering of quasiparticles by the wall of an expanding bubble produced at the electroweak phase transition. In agreement with the recent work of Gavela, Hernández, Orloff and Pène, we conclude that QCD damping effects reduce the asymmetry produced to a negligible amount. We interpret the damping as quantum decoherence. We compute the asymmetry analytically. Our analysis reflects the observation that only a thin, outer layer of the bubble contributes to the coherent scattering of the quasiparticles. The generality of our arguments rules out any mechanism of electroweak baryogenesis that does not make use of a new source of CP violation.

Submitted to: *Physical Review D*

HEP-PH-9404302

*Work supported by the Department of Energy, contract DE-AC03-76SF00515.

1 Introduction

The present work addresses the possibility of implementing the phase of the CKM mixing matrix of the quarks as the source of CP violation for electroweak baryogenesis.

The origin of the baryon asymmetry of the universe (BAU) is recognized as a fundamental question of modern physics. Although the BAU is a macroscopic property of the entire observable universe, the ingredients for its explanation are contained in the microscopic laws of particle physics, as pointed out by Sakharov [1].

Sakharov established on general grounds that a theory of particle interactions could account for the production of the BAU at an early epoch of the universe, provided that this theory contains B-violating processes which operated in a C- and CP-violating environment during a period when the universe was out of thermal equilibrium.

The state of the art in particle physics is the Standard Model of gauge interactions among quarks and leptons. CP violation has been observed and is thought to originate from the quark mixing matrix. B violation is believed to have taken place through nonperturbative weak-interaction processes in the hot plasma of the early universe.

Kuzmin, Rubakov and Shaposhnikov [2] pointed out that implementing the program of Sakharov in the Standard Model would require the electroweak phase transition to be first order, with the baryon asymmetry being produced at the interface of bubbles of nonzero Higgs expectation value, which expand into the unbroken phase. Furthermore, Shaposhnikov [3] established a stringent upper bound on the Higgs mass by requiring that the resulting baryon asymmetry not be washed out by the B-violating processes from which it originated. The latest studies [4, 5] of the electroweak phase transition have refined this bound to a value which is now ruled out by experiment. Although a better understanding of the nonperturbative sector of the electroweak theory is required, this bound directly challenges the possibility of electroweak baryogenesis.

The above obstacle, however, is not the principal reason which has motivated various groups to enlarge the framework of the Standard Model in the search for a viable scenario of baryogenesis [6]. In the Standard Model, all CP violation results from a single complex phase in the quark mixing matrix. This phase can be transformed away in the limit that any two quarks of equal charge have the same mass, and it can appear in physical observables only through processes which mix all three generations of quarks. These limitations suppress CP-violating effects in the Standard Model for most processes by a factor of the order of 10^{-20}. Given that CP violation is a necessary ingredient for baryogenesis, it is difficult to reconcile this suppression factor with the observed ratio of the baryons per photon in the Universe, $(4\text{–}6) \times 10^{-11}$.

Recently, Farrar and Shaposhnikov (FS) [7] performed a detailed analysis of this important question. Despite all expectations, they concluded that Standard-Model CP violation does not lead to the above suppression; instead, they found that under optimal conditions it is sufficient for generating a ratio of baryons per photon of as much as the observed 10^{-11}. A crucial ingredient of their analysis is the interaction of the quarks with thermal gauge and Higgs bosons in the plasma, which they correctly take into account by expressing the interaction between the quarks and the bubble interface as the scattering of quasiparticles.

Subsequently, Gavela, Hernández, Orloff and Pène (GHOP) raised objections to this analysis [8]. They pointed out that Farrar and Shaposhnikov did not take into account the quasiparticle width (damping rate). The width results from the fast QCD interactions of the quasiparticles with the plasma, and is larger than any other scale relevant to the scattering. They proposed to take the damping into account, and they concluded that it reduces the magnitude of the BAU produced by the FS mechanism to a negligible amount, in agreement with earlier expectations. The details of their analysis will appear in future publications.

We propose a novel interpretation of the damping rate, γ, of a quasiparticle as a measure of its limited quantum coherence. The quasiparticle wave is rapidly damped because the components of the wave are rapidly absorbed by the plasma, and reemitted in a different region of the phase space. This decoherence phenomenon prevents components of the wave from participating in quantum interference over a distance longer than a *coherence length*, ℓ, whose magnitude is proportional to $1/\gamma$. Quantum interference is necessary for the generation of a CP-violating observable.

The above considerations lead us to reexamine the physical mechanism of scattering of a particle off a medium. The latter does not take place at the interface but instead results from the coherent interference of components of the particle wavefunction which are refracted by the bulk of the scattering medium. This observation can be ignored if the incoming wave is coherent for an arbitrary amount of time, but not for a quasiparticle which has a coherence length much shorter than any other relevant scale. This perspective provides a transparent physical understanding of the scattering properties of a quasiparticle off the bubble. The coherent scattering of a quasiparticle effectively takes place only in a very thin outer layer of the bubble, which drastically reduces the probability of reflection.

In order to contribute to a CP-violating observable, a quasiparticle wave must scatter many times in the bubble before it decoheres. It must encounter mixing of all three generations of quarks and the CP-odd phase in the CKM matrix. The scattering takes place

through the quark mass term in the bubble of broken phase, and through interaction with charged Higgs in the plasma. However, the mean free path for each of these scatterings is far longer than the coherence length of the quasiparticle wave. The wave has almost completely died away by the time it has scattered a sufficient number of times. Consequently, the baryon asymmetry produced is insignificant, orders of magnitude smaller than the observed asymmetry (and the asymmetry found by Farrar and Shaposhnikov).

We make the above arguments quantitative by deriving a diagrammatic expansion for the reflection of a quasiparticle wave off a bubble. This expansion expresses a reflection amplitude as a sum of paths in the bubble with various flavor changes and chirality flips, with each path being damped by the exponential of its length expressed in units of the coherence length ℓ. This method provides an analytic expression for the baryon asymmetry and demonstrates that the leading order contributions are proportional to the Jarlskog determinant and to an analogous invariant measure of CP violation. Our analysis corroborates the findings of GHOP that the BAU produced is suppressed to a negligible amount as result of plasma effects.

Our arguments of decoherence are of great generality and rule out any scenario of baryogenesis which implements the phase of the CKM matrix as the sole source of CP violation.

In Section 2, we review the main aspects of the electroweak phase transition which are needed to carry out our analysis and we describe the FS mechanism of baryogenesis. In Section 3, we introduce and justify the concept of the coherence length, and we describe the physics of the scattering which takes into account the limited coherence of the quasiparticles. Using these insights, we describe in Section 4 our method for computing the baryon asymmetry in presence of a sharp bubble wall. We discuss various additional suppressions which occur when the wall has a more realistic thickness. Finally, we summarize our results and discuss their applicability to more general situations. In particular, we briefly discuss possible implications for other scenarios of electroweak baryogenesis.

2 The Mechanism of Farrar and Shaposhnikov

In this section, we review the relevant features of the electroweak phase transition, and we describe the FS mechanism of electroweak baryogenesis.

2.1 The Electroweak Phase Transition

It is well established after the pioneering work of Kirzhnits and Linde [9] that the electroweak $SU(2)\times U(1)$ gauge symmetry was unbroken in the early universe. As the universe cooled down to a temperature of order $T \sim 100\,\mathrm{GeV}$, the thermal expectation value of the Higgs field developed a nonzero value, breaking the electroweak symmetry.

This phase transition is thought to have been a first-order transition, although currently unresolved difficulties related to the non-abelian gauge sector of the thermal plasma have prevented a proof of this statement. Electroweak baryogenesis relies on this assumption in order to meet the criteria of Sakharov. In a second-order phase transition, the departure from thermal equilibrium results from the time dependence of the temperature, which is driven by the expansion of the universe. The rate of expansion of the universe, $H = T^2/M_{\mathrm{Planck}}$, is typically 17 orders of magnitude slower than a typical process in the plasma, far too slow to generate a significant departure from equilibrium. On the other hand, in a first-order phase transition the Higgs VEV jumps suddenly to a nonzero value. This triggers the nucleation of bubbles of broken phase. As a bubble expands, its surface sweeps through the plasma, requiring a given species to suddenly adjust its thermal distribution to its nonzero mass inside the bubble. This produces a temporary state of nonequilibrium with a time scale of the order (thickness)/(velocity)$\sim 10^{1\text{-}3}/T$, which is comparable to the microscopic time scale of the plasma.

The dynamics of bubble expansion are fairly well understood. These bubbles grow to a macroscopic size of order $10^{12}/T$ until they fill up the universe. In contrast, baryogenesis is a microscopic phenomenon $\sim$ (1–100)$/T$. This allows one to ignore complications due to the curvature of the wall by assuming the latter to be planar. The thickness of the interface is of order (10–100)$/T$, depending on the Higgs mass, while the terminal velocity of expansion v_W has been calculated to be non-relativistic [5, 10], with the smallest allowed velocity, of order 0.1, attained in the thin-wall limit. Furthermore, for this range of parameters, the growth of the bubble has been shown to be stable [11].

The above considerations lead to a picture of the electroweak phase transition favorable for the making of the baryon asymmetry.

2.2 The Mechanism of Farrar and Shaposhnikov

Farrar and Shaposhnikov proposed a simple mechanism of baryogenesis based on the observation that as the wall sweeps through the plasma, it encounters equal numbers of quarks and antiquarks which reflect asymmetrically as a result of the CP-violating

interactions [7]. This mechanism leads to an excess of baryons inside the bubble and an equal excess of antibaryons outside the bubble. Ideally, the excess of baryons outside is eliminated by baryon violating processes while the excess inside is left intact, leading to a net BAU.

Outside the bubble is the domain of the unbroken phase. There are rapid B-violating processes which occur at a rate per unit volume of $, _{\rm out} = \kappa(\alpha_W T)^4$. The coefficient κ is not reliably known, but Monte Carlo simulations [12] suggest $\kappa \sim .1$–1. These processes cause the baryon asymmetry to relax to a thermally-averaged value of zero. A fraction of the antibaryon excess escapes annihilation by diffusing back inside the bubble, an effect enhanced by the motion of the wall, and which can be accounted for by solving diffusion equations [7].

Inside the bubble, the known B-violating processes are instanton processes [13], which can be ignored because they occur at a rate smaller than the expansion rate of the universe, and sphaleron processes [2], which occur at a rate $, _{\rm in} \sim \exp(-2g_W\langle\phi\rangle/\alpha_W T)$. In order to prevent the loss of the baryon excess in a subsequent epoch, the latter processes must occur at a rate smaller than the expansion rate of the universe: $, _{\rm in} \ll (T^2/M_{\rm Planck})T^3$. Since the expectation value $\langle\phi\rangle$ behaves parametrically as $1/m_H^2$, this constraint yields an upper bound on the Higgs mass [3, 5] of order 45 GeV, which lies below the current experimental limit of 58 GeV [14]. This conflict is a major difficulty for Standard-Model baryogenesis. It can be resolved either by a drastic reformulation of sphaleron physics or by extending the parameter space of the symmetry-breaking sector. Both avenues are the subject of active investigation.

2.3 Optimal Parameters

The goal pursued by Farrar and Shaposhnikov is to use the CP-violating phase of the quark mixing matrix as the only source of CP violation for the phase separation of baryons. To discuss this aspect, it is useful to eliminate complications due to other aspects of baryogenesis such as the physics of the B-violating processes and the structure of the wall. If it turns out that the mechanism works within this simplified framework, one can reconsider the analysis within the full setting. In the following, we select ideal conditions which not only simplify the analysis but also optimize the generation of the baryon asymmetry and make no reference to transport phenomena.

We choose the following values for the B-violating rates:

$$, _{\rm in} = 0 \ , \qquad , _{\rm out} = \infty \ . \tag{1}$$

The first condition prevents the wash out of the asymmetry inside the bubble. The second instantaneously eliminates the excess of antibaryons directly outside the wall without reference to any diffusion process. These conditions clearly maximize the asymmetry and allow one to express it directly in terms of the velocity of the wall and the reflection coefficients for the scattering of quasiparticles off the bubble.

For the parameters of the wall, we choose

$$\delta_W = 0 \ , \qquad\qquad v_W \sim 0.1 \ . \tag{2}$$

A wall of zero thickness enhances the quantum-mechanical aspects of the scattering of fermions off the bubble. In fact, we will show how various suppression factors develop as the wall thickness increases from 2–3/T to the more realistic value 10–100/T quoted earlier. The limit of small thickness was shown [5, 10] to be the limit of maximal damping of the motion of the wall in the plasma, a situation for which calculations are reliable and yield the above value of v_W.

Finally, following FS, we assume that the scattering effectively takes place in $1 + 1$ dimensions. This choice simplifies the calculation greatly. Its justification relies on the observation that the kinematics of the scattering only involves the component of the momentum perpendicular to the wall. In addition, forward scattering produces a maximal change of helicity of the fermion, which is required to produce an asymmetry. Restoration of the 3-dimensional phase space can only suppress the asymmetry further.

2.4 A Formula for n_B/s

Under the above assumptions, we can derive a simple expression for the "baryon-per-photon ratio," n_B/s.

In the rest frame of the wall, at any given instant there is an equal amount of quarks and antiquarks striking the wall from either side. As a result of CP violation, quarks and antiquarks scatter differently in the presence of the bubble, and become asymmetrically distributed between the broken and unbroken phases. By assumption, the baryon number outside the bubble is immediately eliminated, leaving an equal but opposite baryon number inside the bubble. Therefore the net baryon number produced is minus the thermal average of the baryon number in the unbroken phase. The baryon number in the unbroken phase is the sum of the excess due to baryons from the unbroken phase (u) which reflect off the bubble back into the unbroken phase, and the excess due to baryons transmitted from the broken phase (b) into the unbroken phase. Hence the net baryon

number produced is given by

$$n_B = -\frac{1}{3}\Big\{ \quad \int \frac{d\omega}{2\pi} n_L^u(\omega) \mathrm{Tr}\left[R_{LR}^\dagger R_{LR} - \bar{R}_{LR}^\dagger \bar{R}_{LR}\right] \quad + \quad (L \leftrightarrow R)$$
$$+ \quad \int \frac{d\omega}{2\pi} n_L^b(\omega) \mathrm{Tr}\left[T_{LL}^\dagger T_{LL} - \bar{T}_{LL}^\dagger \bar{T}_{LL}\right] \quad + \quad (L \leftrightarrow R)\Big\} \ . \qquad (3)$$

The factor of $1/3$ is the baryon number of a quark. The quantities R and T are matrices in flavor space that contain the reflection and transmission coefficients. For example, R_{LR}^{fi} is the coefficient of reflection for a left-handed quark of initial flavor i which reflects into a right-handed quark (conserving angular momentum) of final flavor f. $\bar{R}_{LR}$ corresponds to the CP-conjugate processes, that is, right-handed antiquarks reflecting into left-handed antiquarks. T_{LL} and $\bar{T}_{LL}$ contain the transmission coefficients of the corresponding particles approaching the bubble wall from the interior. Expression (3) simplifies greatly after using unitarity, $T_{LL}^\dagger T_{LL} + R_{LR}^\dagger R_{LR} = \mathbb{1}$, and CPT invariance, $R_{RL} = \bar{R}_{LR}$:

$$n_B = \frac{1}{3}\Big\{ \int \frac{d\omega}{2\pi} (n_L^u(\omega) - n_R^u(\omega)) - \int \frac{d\omega}{2\pi} (n_L^b(\omega) - n_R^b(\omega)) \Big\} \times \Delta(\omega) \ , \qquad (4)$$

where $\Delta(\omega) = \mathrm{Tr}[R_{RL}^\dagger R_{RL} - R_{LR}^\dagger R_{LR}] = \mathrm{Tr}[\bar{R}_{LR}^\dagger \bar{R}_{LR} - R_{LR}^\dagger R_{LR}]$. The distributions $n_{R,L}^{u,b}(\omega)$ are Fermi-Dirac distributions boosted to the wall frame:

$$n(\omega) = n_0(\gamma(\omega - \vec{v}_W \cdot \vec{p})) = \frac{1}{e^{\gamma(\omega - \vec{v}_W \cdot \vec{p})/T} + 1} . \qquad (5)$$

For zero wall velocity, all thermal distributions are identical in the wall frame so that contributions to n_B/s in eq. (4) from the broken and unbroken phases cancel each other, as do contributions from the scattering of left- and right-handed particles. The motion of the wall introduces the nonequilibrium conditions required for the generation of the baryon asymmetry. The leading contribution to n_B/s thus appears at first order in v_W. Expanding eq. (5) in powers of v_W, using the value $v_w = 0.1$, and dividing by the entropy density, $s = 2\pi^2 g^* T/45 \simeq 45T$,[1] we find the "baryon-per-photon" ratio produced to be

$$\frac{n_B}{s} \simeq \frac{10^{-3}}{T} \int \frac{d\omega}{2\pi} n_0(\omega)(1 - n_0(\omega)) \frac{(\vec{p}_L - \vec{p}_R) \cdot \hat{v}_W}{T} \times \Delta(\omega) \ + \ \mathcal{O}(v_W^2) \, . \qquad (6)$$

The whole calculation of the baryon asymmetry now reduces to the determination of the left-right reflection asymmetry $\Delta(\omega)$.

[1] g^* is the number of massless degrees of freedom in the plasma ~ 103.

The non-trivial structure of the phase space is contained in the factor $(\vec{p}_L - \vec{p}_R) \cdot \hat{v}_W / T$. This vanishes unless, as discussed in the following subsection, interactions with the W and Z bosons in the plasma are taken into account in the propagation of the quarks; there we will see that $(\vec{p}_L - \vec{p}_R) \cdot \hat{v}_W / T \sim \alpha_W$. In addition, the CP-odd quantity $\Delta(\omega)$ vanishes unless flavor mixing interactions occur in the process of scattering. This requires us to take into account the interactions with the charged W and Higgs bosons in the scattering process. At first, this might appear an insurmountable task. However, Farrar and Shaposhnikov suggested that all the relevant plasma effects can consistently be taken into account by describing the process as a scattering of suitably-defined quasiparticles off the wall.

2.5 Quasiparticles

Quasiparticles are fermionic collective excitations in a plasma. They were studied decades ago in a relativistic context in an e^+-e^- plasma [15]. They were considered for the first time in the QCD plasma by Klimov [16] and Weldon [17]. In the vacuum, a massless spin-1/2 particle with energy ω and momentum $\vec{p}$ has the inverse propagator $S_0^{-1} = \gamma^0 \omega - \vec{\gamma} \cdot \vec{p}$. In the plasma, the particle is dressed, acquiring a thermal self-energy of the form

$$\Sigma(\omega, \vec{p}\,) = \gamma^0 a(\omega, p) - b(\omega, p) \vec{\gamma} \cdot \vec{p}\ . \tag{7}$$

The dispersion relations for the quasiparticles are obtained by solving for the poles of the full propagator, including the self-energy. We need to solve

$$\det[S_0^{-1} - \Sigma(\omega, \vec{p}\,)] = 0\ . \tag{8}$$

The solution is

$$\omega = a(\omega, p) \pm p[1 - b(\omega, p)]\ . \tag{9}$$

The quantity $a(\omega, p)$ has a nonzero value, Ω, at zero momentum, so that there is a mass gap in the dispersion relations. A peculiar feature of this solution is the appearance of two branches as seen in Fig. 1. The upper, "normal" branch (n) corresponds to a "dressed" quark propagating as if it had an effective mass Ω. The second, "abnormal" branch (a) is interpreted [18] as the propagation of a "hole," that is the absence of a antiquark of same chirality but opposite momentum. A "hole" is expected to be unstable at large momentum, but is thought to be stable for relatively small momentum [19], which is the region of momentum of interest in the FS mechanism.

At small quasiparticle momentum, where the largest phase separation of baryons occurs, the self-energy can be linearized as

$$\Sigma(\omega, \vec{p}) \simeq \gamma^0(\Omega - \omega) - \vec{\gamma} \cdot \vec{p}/3 \ . \tag{10}$$

The solutions for the poles in the quasiparticle propagator are in this approximation simply

$$\omega \simeq \Omega \pm \frac{p}{3} \ . \tag{11}$$

Here the factor of $1/3$ is the quasiparticle group velocity, $d\omega/dp$, at zero momentum.

In the hot plasma of the early universe, left- and right-handed quasiparticles acquire distinct thermal masses Ω_L and Ω_R because only left-handed quarks couple to the thermal W bosons. The thermal masses also develop flavor dependence because different flavors couple with different strength to the thermal Higgs bosons. The thermal masses of the left-handed quasiparticles are given explicitly by [17, 7]

$$\Omega_L^2 = \frac{2\pi\alpha_s T^2}{3} + \frac{\pi\alpha_W T^2}{2}\left(\frac{3}{4} + \frac{\sin^2\theta_W}{36} + \frac{M_u^2 + K M_d^2 K^\dagger}{4M_W^2}\right) \ , \tag{12}$$

where the contributions from thermal interactions with gluons, electroweak gauge bosons, and Higgs bosons are all apparent. In this expression, K is the CKM matrix, $M_u = \mathrm{diag}(m_u, m_c, m_t)$, $M_d = \mathrm{diag}(m_d, m_s, m_b)$, and the Yukawa couplings to the Higgs have been related to the masses of the quarks and the W in the broken phase. For right-handed up quarks,

$$\Omega_R^2 = \frac{2\pi\alpha_s T^2}{3} + \frac{\pi\alpha_W T^2}{2}\left(\frac{4\sin^2\theta_W}{9} + \frac{M_u^2}{M_W^2}\right) \ , \tag{13}$$

while for right-handed down quarks,

$$\Omega_R^2 = \frac{2\pi\alpha_s T^2}{3} + \frac{\pi\alpha_W T^2}{2}\left(\frac{\sin^2\theta_W}{9} + \frac{M_d^2}{M_W^2}\right) \ . \tag{14}$$

These results for the thermal masses hold at leading order in the temperature, T, assuming that T is much larger than any other energy scale. In section 4, we will see that in order to have flavor mixing of right-handed quarks, we need to consider corrections proportional to $\log m/T$ that arise when nonzero quark masses in the broken broken phase are taken into account.

The full structure of the dispersion relations (9) for left- and right-handed particles in the broken and the unbroken phases is depicted in Fig. 2. The graphs which contribute

to the self-energy are of the form shown in Fig. 3a, where the quark interacts with either a gluon, a W boson or a Higgs boson in the plasma. The dominant contribution to the Ω's is left-right- and flavor-symmetric, and comes from gluon exchange diagrams. This is contained in the left-right average of the Ω's which, ignoring the small flavor-dependent pieces from Higgs and hypercharge-boson interactions, is given by

$$\Omega_0 \simeq \frac{g_s T}{\sqrt{6}} \left(1 + \frac{9\alpha_W}{64\alpha_s}\right) \simeq 50\,\mathrm{GeV}\,. \tag{15}$$

Splitting between left- and right-handed excitations comes dominantly from the $W^\pm$ interactions,

$$\delta\Omega = \Omega_L - \Omega_R \simeq \frac{g_W^2 T^2}{20\Omega_0} \simeq 4\,\mathrm{GeV}\,. \tag{16}$$

In the unbroken phase, the energy levels of left- and right-handed quasiparticles intersect at an energy close to Ω_0, at a momentum $|\vec{p}|$ near $(3/2)\delta\Omega$. In the broken phase, level-crossing takes place, leaving a mass gap of thickness equal to the mass of the quark at the core of the quasiparticle. This is shown in Fig. 2. Quasiparticles with such energies cannot propagate in the broken phase; they are totally reflected by the bubble if they approach it from the unbroken phase. This latter property is of crucial importance in the FS mechanism and restricts the relevant phase space to a region near $\omega = \Omega_0$.

Finally, there are other contributions to the self-energy resulting from neutral- and charged-Higgs bosons. Their effects are unimportant for the propagation of a quasiparticle in either phase. However, the self-energy contributions from interactions with the charged Higgs are crucial for the generation of the baryon asymmetry. Without them, the thermal masses would be flavor independent, and in a mass-eigenstate flavor basis, the CKM matrix — the only source of CP violation — would not be present. With the charged-Higgs interactions included, it is impossible to diagonalize the evolution equations for the quasiparticles simultaneously in both phases: the required CP-violating flavor mixing will be present in one or both phases, allowing the separation of the baryons across the bubble wall.

2.6 Phase Separation of Baryon Number

It is known that a CP-violating observable is obtained by interfering a CP-odd phase, $\mathcal{B}$, with a CP-even phase, $\mathcal{A}$, so that, schematically, the asymmetry resulting from the contribution of particles and antiparticles is proportional to

$$|\mathcal{A} + \mathcal{B}|^2 - |\mathcal{A} + \mathcal{B}^*|^2 = -4\mathrm{Im}\,\mathcal{A}\,\mathrm{Im}\,\mathcal{B}\,. \tag{17}$$

This illustrates the role of quantum mechanics in the generation of a CP-odd observable. Farrar and Shaposhnikov proposed to describe the scattering of quasiparticles as completely quantum mechanical, that is, by solving the Dirac equation in the presence of a space-dependent mass term. In particular, they identified the source of the phase separation of baryon number as resulting from the interference between a path where, say, an s-quark (quasiparticle) is totally reflected by the bubble with a path where the s-quark first passes through a sequence of flavor mixings before leaving the bubble as an s-quark. The CP-odd phase from the CKM mixing matrix encountered along the second path interferes with the CP-even phase from the total reflection along the first path. Total reflection occurs only in a small range of energy of width m_s corresponding to the mass gap for strange quarks in the broken phase, as depicted in Fig. 2. This leads to a phase space suppression of order m_s/T. Inserting this suppression into (6) yields the following estimate of the Farrar and Shaposhnikov baryon-per-photon ratio:

$$\begin{aligned} \frac{n_B}{s} &\simeq 10^{-3}\alpha_W \frac{m_s}{T}\bar{\Delta} \\ &\simeq 10^{-7} \times \bar{\Delta}\,. \end{aligned} \tag{18}$$

This estimate requires $\bar{\Delta}$, the energy-averaged value of the reflection asymmetry, to be at least of order 10^{-4} in order to account for the baryon asymmetry of the universe; this value is just barely attained in Ref. [7].

Gavela et al. pointed out that the above analysis ignores the quasiparticle width, or damping rate, embodied by the imaginary part of the self-energy

$$\Sigma = \mathrm{Re}\,\Sigma - 2i\gamma. \tag{19}$$

The width results from the exchange of a gluon with a particle in the plasma, and has been computed at zero momentum as $\gamma \simeq 0.15 g_s^2 T \simeq 20\,\mathrm{GeV}$ [20]. GHOP made the important observation that this spread in energy is much larger than the mass gap $\sim m$ in the broken phase, and as a result largely suppresses $\Delta(\omega)$. Their arguments rely on the analytic continuation in the ω-plane of the coefficients of reflection for quasiparticle scattering.

In the next Section, we describe the role of the damping rate γ in the scattering of a quasiparticle off the bubble from a perspective which provides a clear physical understanding along with an unambiguous computational method.

3 Coherence of the Quasiparticle

3.1 The Coherence Length ℓ

A Dirac equation describes the relativistic evolution of the fundamental quarks and leptons. Its applicability to a quasiparticle is reliable for extracting on-shell kinematic information, but one should be cautious in using it to extract information on its off-shell properties. A quasiparticle is a convenient bookkeeping device for keeping track of the dominant properties of the interactions between a fundamental particle and the plasma. For a quark, these interactions are dominated by tree-level exchange of gluons with the plasma. It is clear that these processes affect the coherence of the wave function of a propagating quark. To illustrate this point, let us consider two extreme situations.

- *The gluon interactions are infinitely fast.* In this case, the phase of the propagating state is lost from point to point. A correct description of the time evolution can be made in terms of a totally incoherent density matrix. In particular, no interference between different paths is possible because each of them is physically identified by the plasma.[2] As a result, no CP-violating observable can be generated and $\Delta(\omega) = 0$.

- *The gluon interactions are extremely slow.* The quasiparticle is just the quark itself and is adequately described by a wavefunction solution of the Dirac equation, which corresponds to a pure density matrix. In particular, distinct paths cannot be identified by the plasma, as the latter is decoupled from the fermion. This situation was implicitly assumed in the FS mechanism. This assumption, however, is in conflict with the role the plasma plays in the mechanism, which is to provide a left-right asymmetry as well as the necessary mixing processes. In addition, this assumption is in conflict with the use of gluon interactions to describe the kinematical properties of the incoming (quasi-)quark.

The actual situation is of course in between the two limits above. The quasiparticle retains a certain coherence while acquiring some of its properties from the plasma. Whether this coherence is sufficient for quantum mechanics to play its part in the making of a CP-violating observable at the interface of the bubble is the subject of the remaining discussion.

[2] Not only is the quantum mechanics of interference suppressed, but also the scattering process is entirely classical.

The damping rate γ characterizes the degree of coherence of the quasiparticle. It results from 2-to-2 processes of the type shown in Fig. 3b. It is a measure of the spread in energy, $\Delta E \sim 2\gamma$, which results from the "disturbance" induced by the gluon exchanged between the quark and the plasma. From the energy-time uncertainty relation, $1/(2\gamma)$ is the maximum duration of a quantum mechanical process before the quasiparticle is scattered by the plasma. We define a *coherence length* ℓ as the distance the quasiparticle propagates during this time:

$$\ell = v_g \times \frac{1}{2\gamma} \simeq \frac{1}{6\gamma} \simeq \frac{1}{120\,\mathrm{GeV}} \ , \tag{20}$$

where v_g is the group velocity of the quasiparticle. With this definition, we can easily describe the decoherence that occurs during the scattering off a bubble. Of crucial importance for the remaining discussion, the coherence length of the quasiparticle is much shorter than any other scale relevant to the scattering process:

$$\ell \simeq \frac{1}{T} \ \ll \ \frac{1}{p} \simeq \frac{1}{\delta\Omega} \simeq \frac{20}{T} \ , \ \frac{1}{m_s} \simeq \frac{1000}{T} \ . \tag{21}$$

3.2 A Model for Decoherence

Having identified the limited coherence of a quasiparticle, we need to describe its impact on the physics of scattering by a bubble of broken phase. To understand this impact, let us first consider a familiar example, the scattering of light by a refracting medium.

According to the microscopic theory of reflection of light, the refracting medium can be decomposed into successive layers of scatterers which diffract the incoming plane wave. The first layer scatters the incoming wave as a diffracting grid. Each successive layer reinforces the intensity of the diffracted wave and sharpens its momentum distribution. As more layers contribute to the interference, the diffracted waves resemble more and more the full transmitted and reflected waves. This occurs only if the wave penetrates the wall *coherently* over a distance large compared to its wavelength k^{-1}.

In analogy with the microscopic theory of reflection of light by a medium, we can slice the bubble into successive layers which scatter the incoming wave. The wavefunction for a quasiparticle reflected from the bubble is the superposition of the waves reflected from each of the layers. However, the decoherence of the quasiparticles arising from collisions with the plasma implies that quasiparticles reflected from deep inside the bubble back into the symmetric phase cannot contribute coherently to the reflected, outgoing wave of quasiparticles. Having traveled several coherence lengths through the plasma, a

component of the wave reflected from deep inside the bubble will have been repeatedly absorbed and reemitted by the plasma. Each component thereby acquires a distinct momentum and energy, preventing quantum interference of their amplitudes. Therefore, scattering from layers of the bubble deeper than one coherence length does not contribute significantly to the production of a coherent outgoing wave.

We can make the above arguments more specific in three different but complementary ways:

- The scattering occurs because of the gain in mass by the quark when it enters the broken phase; this increment of mass is very small, and the full scattering requires the *coherent* contribution of scatterers up to a distance $1/m$ into the bubble in order for the latter to probe the energy of the wave with a resolution smaller than m. This requirement is not satisfied since, from (21), this minimal penetration length is 3 orders of magnitude larger than the coherence length of the incoming wave.

- From a corpuscular point of view, since scattering in the bubble is due to the quark mass m, the mean free path for scattering is $1/m$. This is 1000 times longer than the coherence length. Therefore the probability for quasiparticle scattering even once in the bubble before it decoheres is extremely small, of order $(m\ell)^2 \sim 10^{-6}$.

- Farrar and Shaposhnikov found a sizable baryon asymmetry generated in an energy range of width m_s where a strange quark is *totally* reflected from the bubble. This energy range corresponds to the mass gap in the broken phase described previously (Fig. 2). However, strange quarks can easily tunnel through a barrier of thickness $\ell \ll 1/m_s$, since they are off-shell by an energy $\Delta\omega \simeq m_s$ for a time $\Delta t \simeq \ell/v_g = 1/(2\gamma)$. Because $\Delta\omega\Delta t = m_s/(2\gamma) \ll 1$, tunneling is completely unsuppressed and the amplitude of the reflected strange-quark wave is only of order $m_s/\gamma \sim 1/1000$.

The probability of scattering several times in the bubble, as is required in order to generate a CP-violating, baryon asymmetry, is thus vanishingly small. The baryon asymmetry results from interference of reflected waves and necessarily involves several flavor-changing scatterings inside the bubble in order to pick up the CP-violating phase of the CKM matrix. We therefore expect that the baryon asymmetry produced when decoherence is properly taken into account will be smaller than the amount found by Farrar and Shaposhnikov by several factors of $m\ell$.

From these physical considerations, we can easily elaborate quantitative methods of computing the scattering off a bubble by quasiparticles with a finite coherence length ℓ.

A simple model is obtained by expressing that when a quasiparticle wave reaches a layer a distance z into the bubble, its amplitude will have effectively decreased by a factor $\exp(-z/2\ell)$. A component which reflects from this layer and contributes to the reflected wave will have decreased in amplitude by another factor of $\exp(-z/2\ell)$ by the time it exits through the bubble wall. We can take this into account by replacing the step-function bubble profile with an exponentially decaying profile:

$$\hat{M}(z) = \begin{cases} Me^{-z/\ell}, & z > 0 \\ 0, & z < 0 \end{cases} . \tag{22}$$

This automatically attenuates the contribution to the reflected wave from layers of the bubble deeper than one coherence length. The analog in the theory of light scattering is the scattering of a light ray by a soap bubble. For this reason, we refer to this model as the "soap bubble" model. It is clear that truncating the bubble in this way renders the bubble interface transparent to the quasiparticle, that is, significantly reduces the amplitude of the reflected wave.

A more rigorous method of computing $\Delta(\omega)$ which we develop in detail in the next Section is to solve an effective Dirac equation in the presence of the bubble, including the decoherence (damping) that results from the imaginary part of the quasiparticle self-energy. We extract Green's functions which allows us to construct all possible paths of the quasiparticles propagating in the bulk of the bubble with chirality flips and flavor changes, each path being damped by a factor $\exp(-\mathcal{L}/2\ell)$ where $\mathcal{L}$ is the length of the path. Paths occurring within a layer of thickness ℓ dominate the reflection amplitudes, in agreement with the previous considerations. We refer to this method as the "Green's function" method.

We have computed $\Delta(\omega)$ using both methods. They give results qualitatively and quantitatively in close agreement. The principal difference is the following: The "soap bubble" model totally ignores scattering off the region deep inside the bubble, and does not take into account small effects from decoherence in the foremost layer. In the next Section we develop the "Green's function" method in detail. The results are summarized in the final Section.

4 Calculation of $\Delta(\omega)$ Including Decoherence

4.1 Dirac Equation for Quasiparticle Scattering

In the unbroken phase where quarks are massless, quasiparticles propagate with a well-defined chirality, and the wavefunctions L and R of left- and right-handed quasiparticles evolve independently according to

$$\begin{aligned} (\omega + \vec{\sigma}\cdot\vec{p} - \Sigma_L(\omega,\vec{p}))L &= 0 \ , \\ (\omega - \vec{\sigma}\cdot\vec{p} - \Sigma_R(\omega,\vec{p}))R &= 0 \ , \end{aligned} \tag{23}$$

where ω and $\vec{p}$ are the energy and momentum of the quasiparticle, and $\Sigma_{L,R}$ are the thermal self-energies discussed in Section 2.5. The largest contribution to quasiparticle reflection and the phase separation of baryons occurs at small momenta where the momenta of left- and right-handed quasiparticles are not significantly different. At small momenta, the self-energies can be linearized (10) as $\Sigma_{L,R} \simeq 2(\Omega_{L,R} - i\gamma) - \omega \pm \vec{\sigma}\cdot\vec{p}/3$. Here $\Omega_{L,R}$ are the thermal masses of left- and right-handed quasiparticles introduced in eqs. (12, 13, 14), and we have included the imaginary damping term (19).

In the bubble of broken phase, the nonzero mass couples the two chiralities of quasiparticles. For an idealized bubble with a wall of zero thickness at $z = 0$ and extending to $z = +\infty$, the mass term is just $M\theta(z)$, where M is the matrix of broken-phase quark masses. The propagation and scattering of the quasiparticles in the presence of the bubble of broken phase is thus governed by an effective Dirac equation,

$$0 = \begin{pmatrix} 2[\omega - \Omega_L + i\gamma + \frac{1}{3}i\vec{\sigma}\cdot\vec{\partial}] & M\theta(z) \\ M^\dagger\theta(z) & 2[\omega - \Omega_R + i\gamma - \frac{1}{3}i\vec{\sigma}\cdot\vec{\partial}] \end{pmatrix} \Psi(z) \ , \tag{24}$$

where $\Psi = \begin{pmatrix} L \\ R \end{pmatrix}$. The field Ψ can be either the field of the down quarks, (d,s,b), or the field of the up quarks (u,c,t), and in either case is a 3-component spinor in flavor space. We ignore the small corrections to this equation induced by boosting to the frame of the bubble wall since they contribute at higher order in the wall velocity. In a flavor basis which diagonalizes Ω_L, this Dirac equation is flavor-diagonal in the symmetric phase ($M\theta(z) = 0$). Inside the bubble however, flavors mix via the mass matrix, which is off-diagonal in such a basis. We treat the mass matrix as a perturbation in order to make the calculation of the quasiparticle reflection coefficients as physically transparent as possible. This is an excellent approximation for all quarks other than the top, for which

$m_t \ell \sim 1$. We will therefore concentrate on the scattering of down quarks in this Section, and describe qualitatively how these results would be altered for the scattering of the top quark. The large top mass does not alter the implications of quasiparticle decoherence for the generation of a baryon asymmetry.

Multiplying the above Dirac equation by 3/2, it becomes

$$\begin{pmatrix} P_L + i\vec{\sigma}\cdot\vec{\partial} & \mathcal{M}\theta(z) \\ \mathcal{M}^\dagger\theta(z) & -(P_R + i\vec{\sigma}\cdot\vec{\partial}) \end{pmatrix} \Psi(z) = 0 \ , \tag{25}$$

where P_L and P_R are the symmetric-phase complex momenta of the left- and right-handed quasiparticles, including the imaginary damping terms,

$$P_L = 3(\omega - \Omega_L + i\gamma) \tag{26}$$

$$P_R = -3(\omega - \Omega_R + i\gamma) \ . \tag{27}$$

The rescaled mass $\mathcal{M}$ is just given by $\mathcal{M} \equiv 3M/2$. We can decompose $P_{L,\,R}$ into the physical (hermitian) momenta $p_{L,\,R}$, and damping terms inversely proportional to the coherence length $\ell = 1/(6\gamma)$ introduced in eq. (20):

$$P_L = p_L - \frac{i}{2\ell} \quad , \quad p_L = 3(\omega - \Omega_L) \ ; \tag{28}$$

$$P_R = p_R + \frac{i}{2\ell} \quad , \quad p_R = -3(\omega - \Omega_R) \ . \tag{29}$$

The damping of the quasiparticle waves due to the imaginary parts of P_L and P_R will be discussed shortly.

As discussed above, we restrict our attention to quasiparticles with momenta perpendicular to the bubble wall. Referring to the components of Ψ as

$$\Psi = \begin{pmatrix} \psi_1 \\ \psi_2 \\ \psi_3 \\ \psi_4 \end{pmatrix} \ , \tag{30}$$

we introduce spinors χ and $\tilde{\chi}$ for quasiparticles with $j_z = \mp 1/2$, where j_z is the z-component of their angular momentum:

$$\chi \equiv \begin{pmatrix} \psi_1 \\ \psi_3 \end{pmatrix} \ ; \tilde{\chi} \equiv \begin{pmatrix} \psi_4 \\ \psi_2 \end{pmatrix} \ . \tag{31}$$

Because of angular momentum conservation, the Dirac equation for Ψ decomposes into two uncoupled equations, one for $j_z = -1/2$ quasiparticles contained in χ,

$$-i\partial_z \chi(z) = \begin{pmatrix} P_L & \mathcal{M}\theta(z) \\ -\mathcal{M}^\dagger\theta(z) & P_R \end{pmatrix} \chi(z) \ , \tag{32}$$

and another for the $j_z = +1/2$ quasiparticles contained in $\tilde{\chi}$,

$$-i\partial_z \tilde{\chi}(z) = \begin{pmatrix} -P_R & \mathcal{M}^\dagger\theta(z) \\ -\mathcal{M}\theta(z) & -P_L \end{pmatrix} \tilde{\chi}(z) \ . \tag{33}$$

In each of χ and $\tilde{\chi}$, the upper component represents a quasiparticle moving towards the wall from the symmetric phase. The lower component represents a quasiparticle reflecting off the bubble back into the symmetric phase. The $j_z = -1/2$ equation describes a left-handed quasiparticle reflecting into a right-handed quasiparticle; the $j_z = +1/2$ equation describes the reversed process.

In the following we concentrate entirely on the scattering of $j_z = -1/2$ quasiparticles contained in χ. To obtain analogous results for the scattering of $j_z = +1/2$ quasiparticles, we need only interchange $P_L \leftrightarrow -P_R$ and $\mathcal{M} \leftrightarrow \mathcal{M}^\dagger$, as is apparent from eqs. (32) and (33).

Consider the equation of motion for $\chi(z)$, eq. (32), keeping in mind the expressions for $P_{L,R}$ in (28, 29). As stated above, P_L and P_R are the symmetric-phase momenta of the left- and right-handed quasiparticles in χ. The signs of the real parts of either P_L or P_R depend on whether the quasiparticle is on the normal or abnormal branches, and this in turn depends on the value of ω (see Fig. 1). (For example, if $\Omega_R < \omega < \Omega_L$, the left-handed quasiparticle is on the abnormal branch and has negative momentum. The right-handed quasiparticle is in this case normal, but also has negative momentum.) What is essential though, is that the sign of the group velocities is independent of energy: the left-handed quasiparticles move toward the bubble and positive z, and the right-handed quasiparticles moves away from the bubble and in the direction of negative z.

Now examine the imaginary parts of P_L and P_R. A left-handed quasiparticle, which moves towards *positive* z, has a momentum with a *positive* imaginary part. Therefore the wavefunction for left-handed quasiparticles decays as $\exp(-z/2\ell)$ as the quasiparticles move towards positive z. A right-handed quasiparticle, which moves toward *negative* z, has a momentum with a *negative* imaginary part. Hence the wavefunction for right-handed quasiparticles decays as $\exp(-|z|/2\ell)$ as the quasiparticles move towards negative z. In other words, the quasiparticles are damped no matter in which direction they propagate.

Note that we have implicitly chosen ω to be real. With this choice, the momenta must become complex in order to satisfy the dispersion relations, and propagation of quasiparticles in space is damped. We have taken ω to be real because energy is conserved in the scattering process. We can then just ignore the factor $\exp(-i\omega t)$ which describes the time dependence of the quasiparticle wavefunction, since it does not affect the probabilities of reflection.

We could have satisfied the dispersion relations with real momenta if we had allowed ω to be complex. Then we could have observed the decay of the quasiparticles in a time $1/(2\gamma)$. But then the reflection probabilities would have an exponentially decaying time dependence, which would require us to study the time and space dependence of quasiparticle scattering in order to determine the time it takes for a quasiparticle to scatter off the bubble.

4.2 Diagrammatic Calculation of Reflection Coefficients

We now derive a perturbative expansion for the reflection coefficients. The result is what one would intuitively expect: a left-handed quasiparticle propagates toward positive z until its velocity is reversed by scattering in the bubble — an insertion of the quark-mass matrix — and then becomes a right-handed quasiparticle, propagating towards negative z, perhaps exiting the bubble and contributing to the reflected quasiparticle wave, or possibly scattering again, and once more propagating as a left-handed deeper into the bubble. Throughout, the quasiparticle wave is damped. To generate a phase separation of baryons, the quasiparticle wave must suffer a sufficient number of scatterings inside the bubble, both with the neutral Higgs condensate, which gives factors of the quark-mass matrix, and with charged Higgs in the plasma, in order to produce a CP-violating observable.

First consider the propagation of quasiparticles in the symmetric phase (again, restricting our attention to the $j_z = -1/2$ quasiparticles contained in χ). For the left- and right-handed quasiparticles contained in χ we need to find Green's functions G_L and G_R satisfying

$$(-i\partial_z - P_{L,R})G_{L,R}(z - z_0) = \mathbb{1}\,\delta(z - z_0) \ . \tag{34}$$

In addition we require the boundary conditions

$$G_L(-\infty) = G_R(+\infty) = 0 \ , \tag{35}$$

which state that there are no sources of quasiparticles at spatial infinity. The unique

solution is

$$G_L(z-z_0) = i\theta(z-z_0)e^{iP_L(z-z_0)} = i\theta(z-z_0)e^{-(z-z_0)/2\ell}e^{ip_L(z-z_0)} , \quad (36)$$
$$G_R(z-z_0) = -i\theta(z_0-z)e^{iP_R(z-z_0)} = -i\theta(z_0-z)e^{-(z_0-z)/2\ell}e^{ip_R(z-z_0)} . \quad (37)$$

The θ-functions indicate that left-handed quasiparticles move toward positive z while the right-handed quasiparticles move toward negative z, as expected. We have substituted the expressions for $P_{L,R}$ (28, 29) to demonstrate that quasiparticle propagation is damped.

Now introduce the quark-mass terms in the bubble as a perturbation, and consider the reflected wave of right-handed quasiparticles at $z = 0$ due to a delta-function source of left-handed quasiparticles at $z = 0$. Let

$$\chi = \begin{pmatrix} \chi_L \\ \chi_R \end{pmatrix} . \quad (38)$$

We thus need to solve (32)

$$(-i\partial_z - P_L)\chi_L(z) = -i\delta(z)\chi_L(0) + \mathcal{M}\theta(z)\chi_R(z) , \quad (39)$$
$$(-i\partial_z - P_R)\chi_R(z) = -\mathcal{M}^\dagger\theta(z)\chi_L(z) . \quad (40)$$

From the equations satisfied by the Green's functions we see that the solution is given by

$$\chi_L(z) = -iG_L(z)\chi_L(0) + \int dz_0 G_L(z-z_0)\mathcal{M}\theta(z_0)\chi_R(z_0) , \quad (41)$$
$$\chi_R(z) = \int dz_0 G_R(z-z_0)(-\mathcal{M}^\dagger)\theta(z_0)\chi_L(z_0) , \quad (42)$$

where the integrals are over all z_0. These expressions can be iterated to find the reflected wave to any order in the quark mass matrix.

The reflection matrix R_{LR}, where the subscript indicates that left-handed quasiparticles are reflected into right-handed quasiparticles, is obtained by considering all possible flavors of initial and final quasiparticles. For example, R^{fi}_{LR}, the reflection coefficient for scattering of initial flavor i into a final flavor f, is found by calculating the f-component of $\chi_R(0)$ when the i-component of $\chi_L(0)$ is set equal to one and the other components are set to zero. From the solution eq. (42), we see that the reflection matrix is given by the expansion

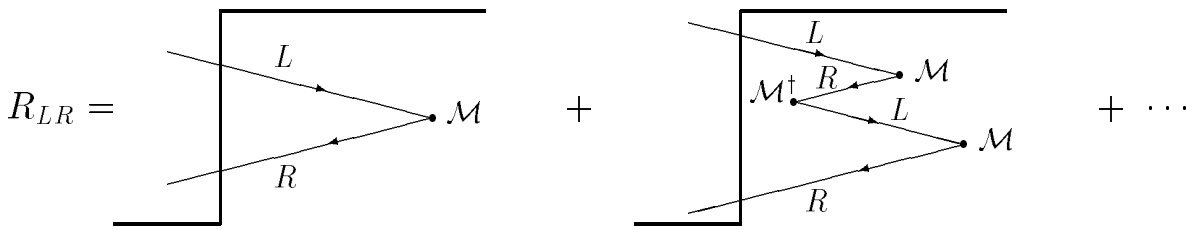

Figure 4: First two terms in the expansion for the reflection matrix R_{LR}. The bubble of broken phase is indicated by the step. An incident left-handed quasiparticle approaches the bubble from the left, and is scattered by the quark-mass term $\mathcal{M}$ in the bubble, becoming a right-handed quasiparticle which moves back towards the bubble wall. The right-handed particle can then exit the bubble and contribute to the reflected wave, or else can scatter again, via $\mathcal{M}^\dagger$, leading to a contribution to the reflected wave at higher order in the quark mass matrix. The full reflected wave is obtained by summing up these diagrams and integrating over the positions of the scatterings in the bubble.

$$
\begin{aligned}
R_{LR} &= -i \int dz_1 G_R(-z_1)(-\mathcal{M}^\dagger)\theta(z_1) G_L(z_1) \\
&- i \int dz_1 dz_2 dz_3 G_R(-z_3)(-\mathcal{M}^\dagger)\theta(z_3) G_L(z_3 - z_2)\mathcal{M}\theta(z_2) G_R(z_2 - z_1)(-\mathcal{M}^\dagger)\theta(z_1) G_L(z_1) \\
&\quad + \cdots \qquad (43) \\
&= i \int_0^\infty dz_1 e^{-iP_R z_1} \mathcal{M}^\dagger e^{iP_L z_1} \\
&+ i \int_0^\infty dz_1 \int_{z_1}^0 dz_2 \int_{z_2}^\infty dz_3 \; e^{-iP_R z_3} \mathcal{M}^\dagger e^{iP_L (z_3 - z_2)} \mathcal{M} e^{iP_R (z_2 - z_1)} \mathcal{M}^\dagger e^{iP_L z_1} + \cdots \; . \qquad (44)
\end{aligned}
$$

This expansion is shown diagrammatically in Fig. 4.

Let us now make explicit the damping of the quasiparticle waves. Decomposing each of P_L and P_R into a momentum and a damping term as in eqs. (28, 29), the previous expression for R_{LR} becomes

$$
\begin{aligned}
R_{LR} &= i\int_0^\infty dz_1 e^{-z_1/\ell} e^{-ip_R z_1}\mathcal{M}^\dagger e^{ip_L z_1} \\
&+ i\int_0^\infty dz_1 \int_{z_1}^0 dz_2 \int_{z_2}^\infty dz_3 \exp[-(z_1+|z_2-z_1|+|z_3-z_2|+z_3)/(2\ell)] \\
&\times e^{-ip_R z_3}\mathcal{M}^\dagger e^{ip_L(z_3-z_2)}\mathcal{M} e^{ip_R(z_2-z_1)}\mathcal{M}^\dagger e^{ip_L z_1} + \cdots \ . \qquad (45)
\end{aligned}
$$

The quasiparticle wave is evidently damped along each leg of its trajectory. The overall suppression for each term in R_{LR} is just $\exp(-\mathcal{L}/2\ell)$, where $\mathcal{L}$ is the distance traveled by a quasiparticle in the barrier. In particular, it is apparent that there will be no significant contribution to R_{LR} from paths which travel to a depth of more than one coherence length into the bubble. Hence only an extremely thin outer layer of the bubble contributes to the coherent reflected wave.

This perturbative expansion for the reflection matrix R is the basis for the calculations we are about to describe. We will work throughout to lowest nonvanishing order in the quark mass matrix. This expansion is valid as long as $M\ell \ll 1$. This condition is easily satisfied for all quarks other than the top, for which the expansion parameter is of order unity, and for which our results will only be qualitative.

We also work to lowest order in the $\mathcal{O}(\alpha_W)$ flavor-dependent terms in $p_{L,R}$ that arise from Higgs contributions to the thermal self-energy. Decompose $p_{L,R}$ as

$$
p_L = p_L^0 \mathbb{1} + \delta p_L \ , \qquad (46)
$$

$$
p_R = p_R^0 \mathbb{1} + \delta p_R \ , \qquad (47)
$$

where $p_{L,R}^0$ contain the large, flavor-independent terms in $p_{L,R}$, while $\delta p_{L,R}$ are proportional to the $\mathcal{O}(\alpha_W)$, flavor-dependent pieces in $\Omega_{L,R}^2$ that arise from interactions with Higgs. Examining the expression (12) for Ω_L^2, and formula (28) for p_L, we see that for down quarks, δp_L is given in a mass-eigenstate flavor basis by

$$
\delta p_L \simeq -\frac{3\pi\alpha_W T^2}{16\Omega_0}\frac{K^\dagger M_u^2 K + M_d^2}{M_W^2} \ . \qquad (48)
$$

For the scattering of up quarks, M_d and M_u are interchanged, as are K and $K^\dagger$. The non-commutativity of δp_L with $\mathcal{M}$ gives rise to flavor mixing in the broken phase.

The thermal masses Ω_R^2 for right-handed quarks are flavor-diagonal when approximated for large temperatures, T (13, 14). Hence in this approximation, p_R is diagonal and does not contribute to the flavor mixing required for CP violation. In the broken

phase, the quarks appearing in the self-energy graphs are massive, and Ω_R^2 acquires off-diagonal terms (which are usually neglected at large temperatures). As pointed out by GHOP, the resulting off-diagonal terms in δp_R, which do not commute with the quark mass matrix, lead to additional contributions to $\Delta(\omega)$. For down quarks,

$$\delta p_R = \cdots + \frac{3\alpha_W}{32\pi\Omega_0} \frac{M_d K^\dagger M_u^2 \log(M_u^2/T^2)\, K M_d}{M_W^2} + \cdots \,, \tag{49}$$

where we have omitted the flavor-independent terms of order T^2. All masses are high-temperature, broken-phase masses. Again, for the scattering of up quarks, $M_d \leftrightarrow M_u$ and $K \leftrightarrow K^\dagger$.

In addition to working to lowest nonvanishing order in the quark-mass matrix $\mathcal{M}$, we also work to lowest order in $\delta p_{L,R}$, which is equivalent to lowest nonvanishing order in α_W. Given that in the range of momentum where our analysis is applicable the diagonal components of $p_{L,R}$ are much smaller than $1/\ell$, we could justifiably work to lowest order in $p^0_{L,R}$ as well. However, we list results valid to all orders in $p^0_{L,R}$ in order to show the energy dependence of $\Delta(\omega)$.

We find two leading contributions to $\Delta(\omega)$. The first contribution is the dominant contribution when quark masses are neglected when calculating the self-energy in the broken phase. In this case δp_R in eq. (47) is diagonal and commutes with the quark mass matrix. This is the only contribution considered by FS, and comparing our results with FS we can see the dramatic effect of decoherence. In a second calculation, we calculate the contribution to $\Delta(\omega)$ that comes from including the off-diagonal terms in δp_R. GHOP found the largest contribution to $\Delta(\omega)$ when considering the scattering of up-type quarks with these terms included. In each case we take into account the finite coherence length of the quasiparticle by using expansion (44) for the coefficient of reflection.

4.3 Calculation of $\Delta(\omega)$ Neglecting δp_R

The leading contribution to $\Delta(\omega)$ when δp_R is ignored appears at $\mathcal{O}(\mathcal{M}^6)$. In this case the momentum of the right-handed quasiparticles is diagonal and commutes with the quark-mass matrix. Then the expression for R_{LR}, eq. (44), can be written as

$$\begin{aligned} R_{LR} &= i\int_0^\infty dz_1 \mathcal{M} e^{-z_1/\lambda} \\ &+ i\int_0^\infty dz_1 \int_{z_1}^0 dz_2 \int_{z_2}^\infty dz_3\, \mathcal{M} e^{-(z_3-z_2)/\lambda} \mathcal{M}^2 e^{-z_1/\lambda} + \cdots \,, \end{aligned} \tag{50}$$

where $1/\lambda = 1/\ell - i(p_L - p_R^0)$. For simplicity, we have chosen a mass-eigenstate basis where $\mathcal{M}$ is diagonal. Evaluating the integrals, we find that

$$R_{LR} = i\mathcal{M}\lambda(\mathbb{1} - \mathcal{M}^2\lambda^2 + \mathcal{M}^2\lambda^2\mathcal{M}^2\lambda^2 + \mathcal{M}^2\lambda\mathcal{M}^2\lambda^3 + \cdots) \ . \tag{51}$$

To calculate $\Delta(\omega) = \mathrm{Tr}(\bar{R}_{LR}^\dagger \bar{R}_{LR} - R_{LR}^\dagger R_{LR})$,[3] we need the reflection matrix $\bar{R}_{LR}$ for the scattering of CP-conjugate particles. The CP-conjugate process differs only in that the CKM mixing matrix K is replaced with K^*, which means p_L is replaced with $p_L^* = p_L^T$. Hence the reflection matrix $\bar{R}_{L,R}$ is obtained from $R_{L,R}$ by replacing λ with its transpose. The $\mathcal{O}(\mathcal{M}^2)$ and $\mathcal{O}(\mathcal{M}^4)$ terms cancel out of the difference in $\Delta(\omega)$, so that the leading-order contribution is $\mathcal{O}(\mathcal{M}^6)$:

$$\begin{aligned}\Delta_9(\omega) \ = \ & \mathrm{Tr}[\lambda\lambda^{\dagger 2}\mathcal{M}^2\lambda^\dagger\mathcal{M}^2\lambda^{\dagger 2}\mathcal{M}^2 + \lambda^2\lambda^\dagger\mathcal{M}^2\lambda^2\mathcal{M}^2\lambda\mathcal{M}^2 + \lambda^2\lambda^{\dagger 2}\mathcal{M}^2\lambda\mathcal{M}^2\lambda^\dagger \\ & -\lambda\lambda^{\dagger 2}\mathcal{M}^2\lambda^{\dagger 2}\mathcal{M}^2\lambda^\dagger\mathcal{M}^2 - \lambda^2\lambda^\dagger\mathcal{M}^2\lambda\mathcal{M}^2\lambda^2\mathcal{M}^2 - \lambda^2\lambda^{\dagger 2}\mathcal{M}^2\lambda^\dagger\mathcal{M}^2\lambda] \ , \end{aligned} \tag{52}$$

where $1/\lambda^\dagger = 1/\ell + i(p_L - p_R^0)$. Notice that each factor of the quark mass matrix is accompanied by a factor of $\lambda \simeq \ell$. The product $\mathcal{M}\ell$ is the amplitude for the quasiparticle to scatter through the quark mass term while propagating for one coherence length, which is quite small. To lowest order in δp_L,

$$\Delta_9(\omega) \ = \ 4if_9(\Delta p^0\ell)\,\mathrm{Tr}\left[(\delta p_L)^2\mathcal{M}^4\delta p_L\mathcal{M}^2 - (\delta p_L)^2\mathcal{M}^2\delta p_L\mathcal{M}^4\right]\ell^9 \tag{53}$$

$$= \ -\frac{4i}{3}f_9(\Delta p_0\ell)\,\mathrm{Tr}\left[\mathcal{M}^2,\ \delta p_L\right]^3\ell^9 \ , \tag{54}$$

where $\Delta p^0 \equiv p_L^0 - p_R^0$, and f_9 is an energy-dependent form factor given by

$$f_9(x) = \frac{1}{(1+x^2)^6} \ . \tag{55}$$

The subscripts "9" indicates that this contribution to $\Delta(\omega)$ occurs at 9^{th} order in ℓ. It is the largest contribution to $\Delta(\omega)$ due to down quarks when δp_R is neglected. Again note that for every factor of the quark mass matrix or δp_L, there is an accompanying factor of ℓ. Scattering from either the Higgs condensate or the the charged Higgs in the plasma during one coherence length has a very small probability.

Refering to the diagrammatic expansion in Fig. 4, this $\mathcal{O}(\mathcal{M}^6)$ contribution to $\Delta(\omega)$ evidently can come from the interference of two paths which each have 3 chirality flips

[3]The derivation of eq. (4) for $\Delta(\omega)$ made use of unitarity to relate probabilities of reflection and transmission. With damping, unitarity might seem to violated. However, the damping corresponds to decoherence. Baryon number is still conserved throughout the scattering process.

(via the mass term), or it can come from the interference of a path which has just one chirality flip with a path that has 5 chirality flips. The 3 factors of δp_L are distributed among the left-handed segments of the two paths.

We now substitute expression (48) for δp_L and also $\Delta p^0 \ell \equiv p_L^0 - p_R^0 = (\omega - \Omega_0)/\gamma$, using eqs. (28) and (29), and where $\Omega_0 \simeq 50\,\mathrm{GeV}$ is the left-right average of the flavor-independent pieces of $\Omega_{L,R}$ introduced in eq. (15). Our expression for $\Delta_9(\omega)$ for down quarks becomes

$$\Delta_9^d(\omega) = -4\left(\frac{27\pi\alpha_W T^2}{64\Omega_0 M_W^2}\right)^3 \left[1 + \left(\frac{\omega - \Omega_0}{\gamma}\right)^2\right]^{-6} \det\mathcal{C}\;\ell^9\;, \tag{56}$$

The quantity $\det\mathcal{C}$ is the basis-independent Jarlskog determinant [21],

$$\begin{aligned} \det\mathcal{C} &= i\det[M_u^2, K M_d^2 K^\dagger] \\ &= -2J(m_t^2 - m_c^2)(m_t^2 - m_u^2)(m_c^2 - m_u^2)(m_b^2 - m_s^2)(m_b^2 - m_d^2)(m_s^2 - m_d^2)\;, \end{aligned} \tag{57}$$

where the superscript d indicates that this is the contribution to $\Delta_9(\omega)$ due to the scattering of down quarks. Here J is the product of CKM angles $J = s_1^2 s_2 s_3 c_1 c_2 c_3 \sin\delta \sim 10^{-5}$. Clearly, the largest contribution to $\Delta_9^d(\omega)$ comes from paths involving bottom quarks (either incident, reflected or virtual).

For the scattering of up quarks our expansion in the quark-mass matrix breaks down because of the large mass of the top quark. Because of its large mass, the top quark is far off shell in the broken phase (by $m_t - \Omega_0 \simeq 3\gamma$). We therefore expect that if we did not treat the top mass as a perturbation, the contributions from paths involving the top quark would be smaller than the results obtained here. Our results for the up quarks are thus qualitative, and overestimate their contribution to the asymmetry relative to the contribution of the down quarks.

As mentioned above, results for the scattering of up quarks can be obtained from down-quark results by interchanging M_d with M_u and K with $K^\dagger$. From the definition of the Jarlskog determinant in eq. (57), we see that it changes sign under these interchanges. Hence to lowest order in $\mathcal{M}$, the contribution to $\Delta_9(\omega)$ from up quarks, $\Delta_9^u(\omega)$, differs only by a sign from the down-quark contribution, $\Delta_9^d(\omega)$. If the top were as light as the other quarks, the total contribution to $\Delta_9(\omega)$ would vanish (continuing to ignore the off-diagonal terms in δp_R). Because the top is very heavy the dominant terms in $\Delta_9^u(\omega)$, which come from paths involving top quarks, will be reduced. Therefore, the total contribution to Δ_9, given by $\Delta_9^d + \Delta_9^u$, will not vanish.

We reserve further discussion of this contribution for the final Section, and now describe our calculation of the leading contribution to $\Delta(\omega)$ when the off-diagonal terms in δp_R are considered.

4.4 Calculation of $\Delta(\omega)$ Including δp_R

Because δp_R contains two factors of M, when δp_R is included, we need two fewer factors of the quark-mass matrix in order to form an invariant analogous to the Jarlskog determinant. The leading-order term therefore appears at $\mathcal{O}(M^4)$.

To find $\Delta(\omega)$ when the off-diagonal terms in δp_R in eq. (49) are included, we again use the expansion for R_{LR} in eq. (44). We can no longer directly evaluate the z-integrals because of the noncommutativity of δp_L and δp_R with $\mathcal{M}$. Instead we first expand the integral expression for $\Delta(\omega)$ in powers of δp_L and δp_R, and pick out the lowest-order nonvanishing terms, of order $(\delta p_L)(\delta p_R)$. It is then possible to evaluate the flavor-independent integral coefficient. The resulting contribution to $\Delta(\omega)$, at $7^{\rm th}$ order in ℓ, is

$$\Delta_7(\omega) = -8i\, f_7(\Delta p^0 \ell)\, {\rm Tr}\left[\delta p_L \mathcal{M} \delta p_R \mathcal{M}^3 - \delta p_L \mathcal{M}^3 \delta p_R \mathcal{M}\right] \ell^6 \ , \tag{58}$$

where $f_7(\Delta p^0 \ell)$ is an energy-dependent form factor,

$$f_7(x) = \frac{x}{(1+x^2)^4} \ . \tag{59}$$

Note that $\Delta_7(\omega)$ would vanish if either δp_L or δp_R commuted with $\mathcal{M}$. Unlike $\Delta_9(\omega)$, $\Delta_7(\omega)$ is an *odd* function of Δp^0 and so vanishes at $\Delta p^0 = 0$. This is because in order to discern the CP-odd phase in the CKM matrix, we need a CP-even phase, as is apparent in eq. (17). Examining eq. (45) for R_{LR}, the only sources of relative phases are the factors of the form $\exp(ipz)$. To get a nontrivial CP-even phase, we evidently need an odd number of factors of ip. While the trace in $\Delta_9(\omega)$ contains three δp's, the trace in $\Delta_7(\omega)$ contains just two, so we need a factor of Δp^0 to have a nontrivial CP-even phase.

Because $\Delta_7(\omega)$ is an odd function of Δp^0, it vanishes at $\omega = \Omega_0$, in the middle of the energy range where light quarks are totally reflected. This is where Farrar and Shaposhnikov saw the generation of a large baryon asymmetry, and where on a much smaller scale, $\Delta_9(\omega)$ is peaked. We expect that contributions to the integrated asymmetry from $\omega < \Omega_0$ will largely cancel against contributions from $\omega > \Omega_0$, and leaving a very small contribution to the integrated asymmetry from $\Delta_7(\omega)$ for light quarks.

This contribution to the asymmetry arises from the interference of a path that has three chirality flips with a path having one chirality flip. The factor of δp_L can occur

along any of the left-handed segments of the two paths, and similarly the factor of δp_R can occur along any of the right-handed segments.

Substituting the expressions for $\delta p_{L,\,R}$ for down quarks in eqs. (48, 49), and substituting $\Delta p^0 \ell = (\omega - \Omega_0)/\gamma$ as before, expression (58) for $\Delta_7(\omega)$ simplifies to

$$\Delta_7^d(\omega) = 2 \left(\frac{27 \alpha_W T}{32 \Omega_0 M_W^2} \right)^2 f_7 \left(\frac{\omega - \Omega_0}{\gamma} \right) \mathcal{D}_d \, \ell^6 \ . \tag{60}$$

The superscripts d again indicates that this contribution is due to the scattering of down quarks. The quantity $\mathcal{D}_d$ is an invariant measure of CP violation analogous to the Jarlskog determinant:

$$\begin{aligned} \mathcal{D}_d &= \text{Im Tr} \left[M_u^2 \log M_u^2 \, K \, M_d^4 \, K^\dagger \, M_u^2 \, K \, M_d^2 \, K^\dagger \right] \\ &= J \left[m_t^2 m_c^2 \log \frac{m_t^2}{m_c^2} + m_t^2 m_u^2 \log \frac{m_u^2}{m_t^2} + m_c^2 m_u^2 \log \frac{m_c^2}{m_u^2} \right] \\ &\quad \times (m_b^2 - m_s^2)(m_b^2 - m_d^2)(m_s^2 - m_d^2) \ . \end{aligned} \tag{61}$$

Here we have used $\text{Im}(K_{\alpha j} K_{j\beta}^\dagger K_{\beta k} K_{k\alpha}^\dagger) = J \sum_{\gamma,l} \epsilon_{\alpha\beta\gamma} \epsilon_{jkl}$ [21]. Like the Jarlskog determinant, $\mathcal{D}_d$ vanishes if any two quarks of equal charge have the same mass.

Recall that the Jarlskog determinant (57) simply changes sign under the simultaneous interchanges $M_d \leftrightarrow M_u$ and $K \leftrightarrow K^\dagger$. By contrast, $\mathcal{D}_d$ does not treat the up-quark and down-quark mass matrices symmetrically, and becomes a new quantity, $\mathcal{D}_u$, under these interchanges. This new quantity contains two more powers of m_t, and is roughly -1000 times $\mathcal{D}_d$. Hence the contribution to $\Delta_7(\omega)$ due to up-quark scattering, Δ_7^u, obtained from the down-quark contribution by replacing $\mathcal{D}_d$ with $\mathcal{D}_u$, will be much larger than Δ_7^d. Given that contributions from paths including top quarks should be reduced when the off-shellness of the tops is taken into account, the value for Δ_7^u obtained here serves as an upper bound for Δ_7.

We now discuss our results for $\Delta(\omega)$ and their implications for the size of the baryon asymmetry.

5 Presentation and Discussion of the Results

5.1 Results

In the previous Section we computed the energy-dependent reflection asymmetry $\Delta(\omega)$. This asymmetry is the difference of $\text{Tr} \left[\bar{R}_{LR}^\dagger \bar{R}_{LR} \right]$ and $\text{Tr} \left[R_{LR}^\dagger R_{LR} \right]$, the probabilities for

a left-handed quark and its CP-conjugate to be reflected off the bubble, summed over all quark flavors. We calculated the reflection probabilities by solving an effective Dirac equation including all relevant plasma effects as self-energy corrections, in the presence of the space-dependent mass term.

The real part of the self-energy accounts for the gluon interactions which control the kinematical properties of the quarks. It accounts for the interactions with the W's which differentiate between quarks with different chiralities, as well as interactions with the charged Higgs which provide the flavor-changing processes needed for the generation of a CP-violating observable. These effects are embodied in the concept of quasiparticles which was used in the mechanism of Farrar and Shaposhnikov.

The novelty of our calculation resides in our treatment of the imaginary part of the self-energy. We interpreted the latter as a measure of the coherence of the wave function of the quasiparticle, and we introduced the concept of the coherence length, ℓ. We extracted Green's functions which, in conjunction with chirality flips due to the mass term and flavor changes due to interactions with the charged Higgs, lead to the construction of all possible paths contributing to the reflection coefficients (Fig. 4). It is the interference between these paths which survives in the asymmetry, as expected from the general principles described in Sections 2 and 3. An important feature is that each path has an amplitude proportional to $\exp(-\mathcal{L}/2\ell)$, where $\mathcal{L}$ is the length of the path. This confines the scattering to a layer of thickness ℓ at the surface of the bubble, a property already predicted on physical grounds in Section 3. The asymmetry results from processes which involve a sufficient number of changes of flavor as well as a sufficient number of factors of the quark mass matrix, every one of which brings along a factor of ℓ. Consequently, the asymmetry is suppressed by many powers of $M\ell$, the dimensionless product of the quark-mass matrix and the coherence length of the quasiparticle, ℓ, and powers of $(\delta p_L)\ell$ and $(\delta p_R)\ell$, products of the coherence length with the flavor-dependent terms in the momentum matrices for left- and right-handed quasiparticles.

Specifically, we find the asymmetry dominated by: (i) Contributions at order ℓ^7 from processes involving the scattering of up quarks, with two flavor mixings, proportional to $(\delta p_L)(\delta p_R)$, and given in eq. (60):[4]

$$\Delta_7^u(\omega) \;=\; -16\; f_7\Big(6\ell(\omega-\Omega_0)\Big)\;\mathrm{Im\;Tr}[\delta p_L \mathcal{M}\delta p_R \mathcal{M}^3]\;\ell^9 \tag{62}$$

[4]For our numerical results we set $T = 100\,\mathrm{GeV}$. We take the broken-phase W mass as $M_W = T/2$, and scale the broken-phase quark masses accordingly. We use a generous value for the product of sines and cosines of CKM angles: $J = 5\times 10^{-5}$.

$$= 2\left(\frac{27\alpha_W T}{32\Omega_0 M_W^2}\right)^2 \times f_7\Big(6\ell(\omega-\Omega_0)\Big) \times \mathcal{D}_u\, \ell^6 \qquad (63)$$
$$= 10^{-18}\, f_7\Big(6\ell(\omega-\Omega_0)\Big)\ ,$$

where

$$f_7(x) = \frac{x}{(1+x^2)^4}\ ; \qquad (64)$$

and (ii) Contributions at order ℓ^9 from processes involving the scattering of down quarks, with three flavor mixings, proportional to $(\delta p_L)^3$, and given in eq. (56):

$$\Delta_9^d(\omega) = -8\, f_9\Big(6\ell(\omega-\Omega_0)\Big)\ \mathrm{Im\ Tr}[(\delta p_L)^2\mathcal{M}^4\delta p_L\mathcal{M}^2]\ \ell^9 \qquad (65)$$
$$= -4\left(\frac{27\pi\alpha_W T^2}{64\Omega_0 M_W^2}\right)^3 \times f_9\Big(6\ell(\omega-\Omega_0)\Big) \times \det\mathcal{C}\ \ell^9 \qquad (66)$$
$$= 4\times 10^{-22}\, f_9\Big(6\ell(\omega-\Omega_0)\Big)\ ,$$

where

$$f_9(x) = \frac{1}{(1+x^2)^6}\,. \qquad (67)$$

The contribution to $\Delta_7(\omega)$ from down quarks is $\simeq 10^{-21} f_7\Big(6\ell(\omega-\Omega_0)\Big)$, while the contribution to $\Delta_9(\omega)$ from up quarks is smaller than the down-quark contribution.

Our results for up quarks should be regarded as upper bounds. In the broken phase, the kinematics of the top quark is determined entirely by its large mass, as opposed to the light quarks, whose kinematical properties are dominated by their interaction with the plasma in both phases. The reflection asymmetry is produced in an energy range near where level-crossing occurs, well below the top quark mass. At these energies the top quark can only propagate far off-shell. As discussed in Section 4, this diminishes the amplitude for any path which involves flavor changing from or to the top quark. In consequence, the up-quark contribution to $\Delta_9(\omega)$ is suppressed relative to the down-quark contribution, and the up quark contribution to $\Delta_7(\omega)$ given in eqs. (62) and (63) is an upper bound.

The two contributions $\Delta_7^u(\omega)$ and $\Delta_9^d(\omega)$ decompose naturally into a product of three factors, as given in eqs. (63, 66), each of which reflects an important aspect of the physics involved. Let us consider them separately.

The first factor contains powers of α_W/M_W^2, which originate from the flavor changing insertions δp_L or δp_R on the path of the scattered quasiparticle.

The second factor is an energy-dependent function $f(x)$. Although, the precise form of this function is sensitive to the details of the calculation, its general shape is not. This function is a form factor which reflects the increased likelihood of chirality flips at energies for which the various flavors involved have similar momenta. That occurs in the region of level crossing around $\omega \sim \Omega_0 \simeq 50\,\mathrm{GeV}$ (Fig. 2). The form factor peaks at a value of order one, and have a width of order the quasiparticle width, γ. These properties are apparent in Fig. 5. Note that f_9 is peaked at $\omega = \Omega_0$, while f_7, though centered about the same energy, actually vanishes there as the result of the vanishing of the CP-even phase at that energy, as described in Section 4.4.

Finally, the third terms on the right-hand sides of eqs. (63) and (66) are the Jarlskog determinant $\det \mathcal{C}$ and another CP-violating invariant, $\mathcal{D}_u$, which are given explicitly in eqs. (57) and (61) respectively. They contain the expected dependence on the flavor mixing angles and vanish in the limit where any two quarks with the same charge have equal masses. We have already argued that in general a CP-violating observable such as $\Delta(\omega)$ is the result of quantum interference between amplitudes with different CP-even and CP-odd phases. These physical processes can easily be identified from the structure of the traces in eq. (62) and (65). To do so, we represent each of these traces as a closed fermion path with various mass insertions (M_d) and flavor changing insertions (δp_L and δp_R) in the order they appear in the trace. The mass operator changes the chirality of the quark but not its flavor while the flavor changing operator leaves the chirality intact. Any cut performed across two portions of the loop with opposite chirality, divides the loop into two open paths whose interference contributes to the asymmetry. This is illustrated in Fig. 6. These paths are in one-to-one correspondence with the paths constructed with the Green's functions method elaborated in Section 4.

We now calculate the contributions to n_B/s. The contribution from $\Delta_9^d(\omega)$ is, from eq. (18),

$$\begin{aligned}
\left.\frac{n_B}{s}\right|_9 &\simeq 10^{-3}\,\alpha_W\,\frac{1}{T}\int\frac{d\omega}{2\pi} n_0(\omega)(1-n_0(\omega))\,\Delta_9(\omega) \\
&\simeq 10^{-25}\,\frac{1}{T}\int\frac{d\omega}{2\pi} n_0(\omega)(1-n_0(\omega))\; f_9(6\ell(\omega-\Omega_0)) \qquad (68)\\
&\simeq 2\times 10^{-28}\ . \qquad (69)
\end{aligned}$$

Similarly, for the contribution from $\Delta_7^u(\omega)$ we find[5]

$$\left.\frac{n_B}{s}\right|_7 \simeq -6 \times 10^{-27} \ . \tag{70}$$

Because of the peculiarities of top quark kinematics, we cannot say whether the up quark contribution to n_B/s is in fact larger than the contribution from down quarks given in eq. (69). We therefore quote the result (70) as an upper bound on the magnitude of the integrated asymmetry:

$$\left|\frac{n_B}{s}\right| < 6 \times 10^{-27} \ . \tag{71}$$

In Section 3, we advertised another method of computing the asymmetry using a model in which the essentially infinitely thick bubble is replaced with a thin layer of thickness ℓ. We referred to this model as the "soap bubble" model. This model implements quantum decoherence in scattering in the simplest way and provides an analytic form of the asymmetry which has exactly the same structure as the ones obtained in eq. (63) and (66). In fact, the only difference relative to the results for $\Delta(\omega)$ obtained via the "Green's function" method is that for the "soap bubble" model, the energy-dependent form factors f_7 and f_9 are replaced with form factors $\hat{f}_7(x)$ and $\hat{f}_9(x)$, where

$$\hat{f}_7(x) = \frac{2x}{3} \frac{1 - \frac{1}{243}(23x^2 + 7x^4 - 3x^6)}{(1+x^2)^4(1+(x/3)^2)^3} \ , \tag{72}$$

$$\hat{f}_9(x) = \frac{1}{54}\left\{ \frac{1 - \frac{1}{3}x^2}{[(1+x^2)(1+(x/3)^2)]^3} + \cdots \right\} \ . \tag{73}$$

The terms omitted in $\hat{f}_9(x)$ are of order 1% of the term listed. These form factors differ slightly in form and magnitude from their counterparts obtained via the "Green's function" method, but have the same overall shape. For example, $\hat{f}_9(6\ell(\omega - \Omega_0))$ is peaked at $\omega = \Omega_0$, while $\hat{f}_7(6\ell(\omega - \Omega_0))$ vanishes at that energy. This model leads to a baryon-per-photon ratio comparable in magnitude to the values found in eqs. (69) and (70). We do not present the calculations for this model in order to avoid redundancy.

Our results ought to be compared to the results of Farrar and Shaposhnikov. They calculated $\Delta(\omega)$ without taking into account quasiparticle decoherence. They found a

[5]The corresponding contribution to $n_B/s|_7$ from down quarks is only 10^{-29}. Hence the largest contribution to n_B/s from the scattering of down quarks comes from at $\mathcal{O}(\ell^9)$. For up quarks the $\mathcal{O}(\ell^7)$ contribution to n_B/s is larger than the $\mathcal{O}(\ell^9)$ contribution.

significant baryon asymmetry n_B/s of order 10^{-11} from a region of energy for which the strange quark is totally reflected. Taking into account the decoherence of the quasiparticles, we find such total reflection to be impossible and the asymmetry to be reduced to a negligible amount. This conclusion corroborates the findings of Gavela, Hernández, Orloff and Pène (GHOP) [8].

Finally, we would like to comment on the more realistic situation of quasiparticles interacting with a wall of nonzero thickness. Typically, in the Standard Model and in most of its extensions, the wall thickness δ is of order 10-100/T, much larger than the coherence length $\ell \sim 1/T$ and other typical mean free paths.[6] As the wall thickness increases from 0 to a value a few times ℓ, the increment of mass over the latter distance is reduced by a factor ℓ/δ which has the effect to reducing the reflection probabilities accordingly as a power law. As the thickness increases further to a distance of a few wavelengths $k^{-1} \sim 5/T$, a WKB suppression of order $\exp(-k\delta)$ is expected to turn on and to suppress the process further. Clearly, the interior of a thick wall is not a suitable environment for the occurrence of the subtle quantum-mechanical phenomena which are to take place in order to generate a CP-violating observable.

5.2 Conclusions

We have demonstrated that the FS mechanism operating at the electroweak phase transition cannot account for the baryon asymmetry of the universe. Our conclusions agree with the results obtained in Ref. [8].

Our arguments are powerful enough to establish more generally that the complex phase allowed in the CKM mixing matrix cannot be the source of CP violation needed by any mechanism of electroweak baryogenesis in the minimal Standard Model or any of its extensions. Indeed, the generation of a CP-odd observable requires the quantum interference of amplitudes with different CP-odd and CP-even properties and whose coherence persists over a time of at least $1/m_q$. On the other hand, QCD interactions restrict the coherence time to be at most $\ell \sim 1/(g_s^2 T)$, typically three orders of magnitude too small. It is clear from the interpretation of the Jarlskog determinant or any other CP- violating invariant we gave in Section 5.1 and Fig. 6, that the processes necessarily proceed through interference between amplitudes with multiple flavor mixings and chirality flips; as a result, the asymmetry between quarks and antiquarks appears to be strongly suppressed by many powers of ℓm_q. This line of argument does not rely on the details of the mechanism

[6] Although, according to the authors of ref. [6], the possibility of a thin wall is not ruled out.

considered and can be applied to rule out any scenario of electroweak baryogenesis which relies on the phase of the CKM matrix as the only source of CP violation.

QCD decoherence might be avoided in mechanisms which do not involve light quarks. For example, the effect of decoherence is negligible for the top quark: $\ell m_t \simeq 1$. A mechanism which involves the scattering of only the top quark is viable, but at the cost of introducing a new source of CP violation [22]. Other scenarios based on various extensions of the minimal standard model such as the two-Higgs doublets [23] or SUSY [24] are also negligibly affected by the above considerations.

Although the Standard Model contains all three ingredients required by Sakharov, it proves to be too narrow a framework for an explanation of the baryon asymmetry of our universe.

Acknowledgements

We are grateful to Michael Peskin for helping us formulate our picture of decoherence. We thank Helen Quinn and Marvin Weinstein for helpful discussions.

References

[1] A. D. Sakharov *JETP Lett.* **5** (1967) 24.

[2] V. A. Kuzmin, V. A. Rubakov and M. E. Shaposhnikov, *Phys. Lett.* B 155 (1985) 36.

[3] M. E. Shaposhnikov, *Nucl. Phys.* B 287 (1987) 757.

[4] M. Dine, P. Huet and R. Singleton, Jr., *Nucl. Phys.* B 375 (1992) 625.

[5] M. Dine, P. Huet, R. G. Leigh, A. Linde and D. Linde, *Phys. Lett.* B 283 (1992) 319; *Phys. Rev.* D 46 (1992) 550.

[6] For a review of various attempts see A. G. Cohen, D. B. Kaplan and A. E. Nelson, *Ann. Rev. Nucl. Part. Sci.*, **43** (1993) 27. See also refs. [22, 23, 24].

[7] G. R. Farrar and M. E. Shaposhnikov, *Phys. Rev. Lett.* 70 (1993) 2833; preprint CERN-TH-6734/93, RU-93-11.

[8] M. B. Gavela, P. Hernández, J. Orloff and O. Pène, preprint 1993, CERN 93/7081, LPTHE Orsay-93/48, HUTP-93/48, HD-THEP-93-45.

[9] D. A. Kirzhnits and A. D. Linde, *Phys. Lett.* B 72 (1972) 471.

[10] L. McLerran, B.-H. Liu and N. Turok, *Phys. Rev.* D 46 (1992) 2668.

[11] P. Huet, K. Kajantie, R. G. Leigh, L. McLerran and B.-H. Liu, *Phys. Rev.* D 48 (1992) 2477.

[12] See for example J. Ambjorn, T. Askgaard, H. Porter and M. E. Shaposhnikov, *Phys. Lett.* B 244 (1990) 479; *Nucl. Phys.* B 353 (1991) 346.

[13] A. A. Belavin, A. M. Polyakov, A. S. Schwartz and Yu. S. Tyupkin, *Phys. Lett.* B 59 (1975) 85. G. 't Hooft, *Phys. Rev. Lett.* 37 (1976) 8; *Phys. Rev.* D 14 (1976) 3432.

[14] The Aleph Collaboration, *Phys. Lett.* B 313 (1993) 299.

[15] E. S. Fradkin, "Proceedings, P. N. Lebedev Physics Institute" Vol. 29, 123, Consultants Bureau, New York (1967).

[16] V. V. Klimov, *Sov. Phys. JETP*, **55** (1982) 199.

[17] H. A. Weldon, *Phys. Rev.* D 26 (1982) 1394.

[18] H. A. Weldon, *Phys. Rev.* D 40 (1989) 2410.

[19] V. V. Lebedev and A. V. Smilga, *Annals of Physics*, **202**, 229 (1990) and references therein.

[20] E. Braaten and R. D. Pisarsky, *Phys. Rev.* D 46 (1992) 1829.

[21] C. Jarlskog, *Phys. Rev. Lett.* 55 (1985) 1039; C. Jarlskog in "CP Violation," ed. C. Jarlskog (World Scientific, 1989).

[22] A. G. Cohen, D. B. Kaplan and A. E. Nelson, *Nucl. Phys.* B 373 (1992) 453.

[23] L. McLerran, M. E. Shaposhnikov, N. Turok and M. Voloshin, *Phys. Lett.* B 256 (1991) 451.

[24] M. Dine, P. Huet, R. Singleton, Jr. and L. Susskind, *Phys. Lett.* B 257 (1991) 351.

Figure Captions

Figure 1. Schematic picture of the dispersion relations for a fermionic quasiparticle in a hot plasma. The upper curve represents the normal branch. The lower curve represents the abnormal branch, which corresponds to the propagation of a "hole." The abnormal branch becomes completely unstable when it passes through the light cone $\omega = p$ (dotted line) [19].

Figure 2. Dispersion curves linearized for small momentum p. Because the W and Z bosons in the plasma only interact with left-handed quasiparticles, the dispersion relations for left- and right-handed quasiparticles are distinct. For a given chirality, the dispersion relations are as shown in Fig. 1, with both a normal branch and an abnormal branch. (These curves are only shown for a single, light flavor. The curves for other light flavors would be shifted slightly in energy.) In the unbroken phase, the left-handed abnormal branch intersects the right-handed normal branch; in the broken phase, the nonzero quark mass connects the two chiralities and level crossing occurs, as indicated by the dashed lines (here illustrated for the charm quark). The result is a mass gap with thickness of order the quark mass [7].

Figure 3. a) Graph contributing to the real part of the quasiparticle self-energy. The dashed lines represent either gluons, electroweak gauge bosons, or Higgs bosons from the plasma. These graphs are responsible for the thermal masses Ω of the quasiparticles, shown in Fig. 1. b) Graph describing a collision of a quasiparticle (solid line) with a quark or gluon (dashed line) in the plasma. This graph contributes to the imaginary part of the self-energy, and leads to the decoherence of quasiparticle waves.

Figure 4. First two terms in the expansion for the reflection matrix R_{LR}. The bubble of broken phase is indicated by the step. An incident left-handed quasiparticle approaches the bubble from the left, and is scattered by the quark-mass term $\mathcal{M}$ in the bubble, becoming a right-handed quasiparticle which moves back towards the bubble wall. The right-handed particle can then exit the bubble and contribute to the reflected wave, or else can scatter again, via $\mathcal{M}^\dagger$, leading to a contribution to the reflected wave at higher order in the quark mass matrix. The full reflected wave is obtained by summing up these diagrams and integrating over the positions of the scatterings in the bubble.

Figure 5. The energy-dependent form factors f_7 and f_9, evaluated at $(\omega - \Omega_0)/\gamma = 6\ell(\omega - \Omega_0)$. Note that f_9 is peaked at $\omega = \Omega_0 \simeq 50\,\mathrm{GeV}$, while f_7 vanishes there.

Figure 6. This loop summarizes all the contributions to $\Delta_9(\omega)$, and corresponds to the trace in eq. (65). (An analogous loop summarizes the contributions to $\Delta_7(\omega)$.) The solid blobs represent insertions of δp_L, which describes the mixing of quark flavors through interaction with the charged Higgs bosons. The crosses stand for insertions of the quark mass matrix. The loop is then a trace in flavor space of the product of all the insertions. Any individual contribution to the reflection asymmetry can obtained by cutting across two segments of the loop of opposite chirality. This produces two open paths whose interference contributes to the asymmetry, as shown in the right side of the figure.

HEP-PH 9404302

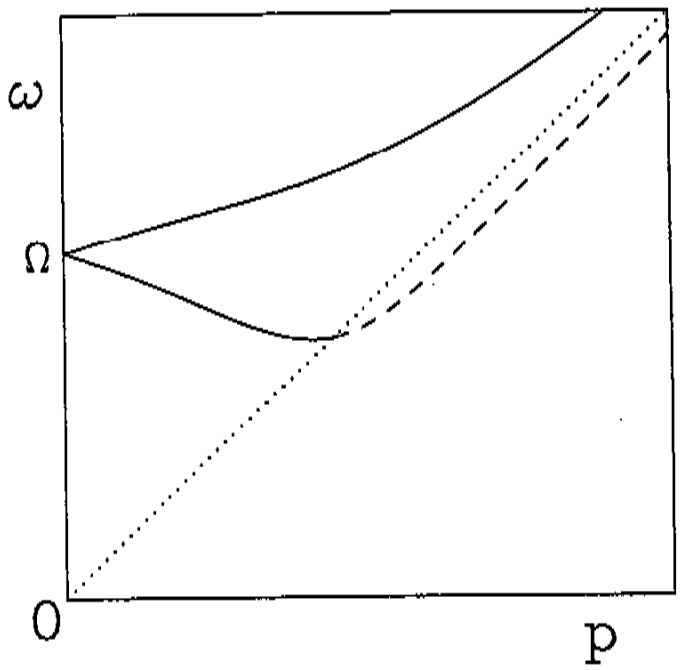

Fig. 1

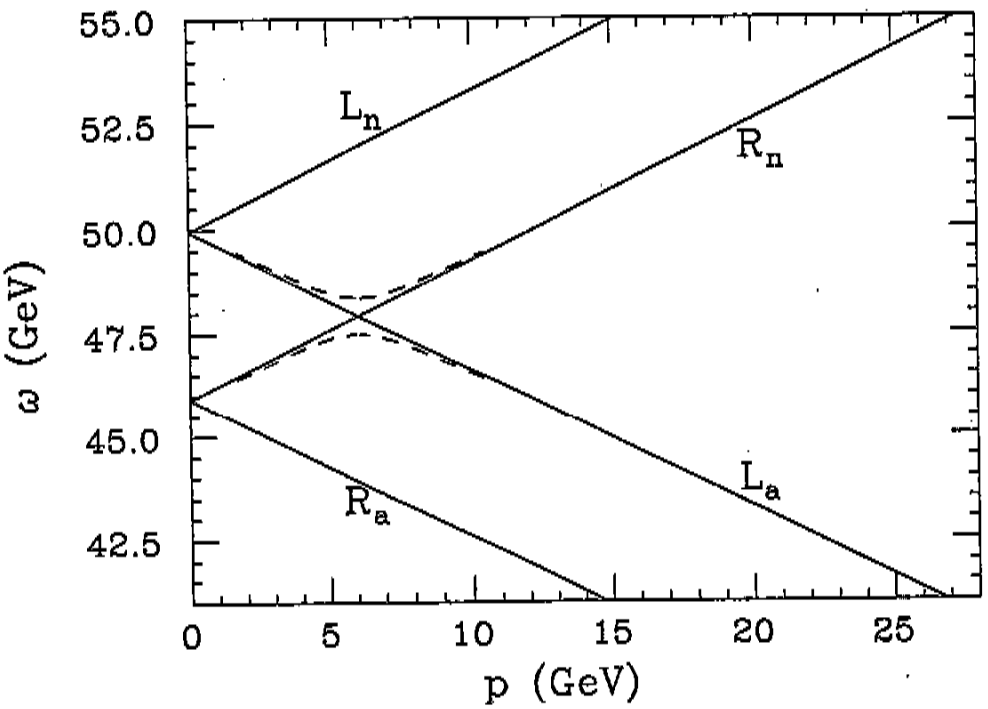

Fig. 2

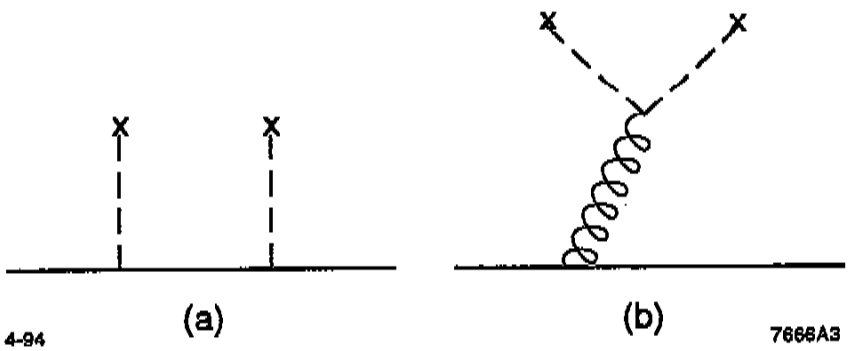
(a)
(b)
4-94
7666A3

Fig. 3

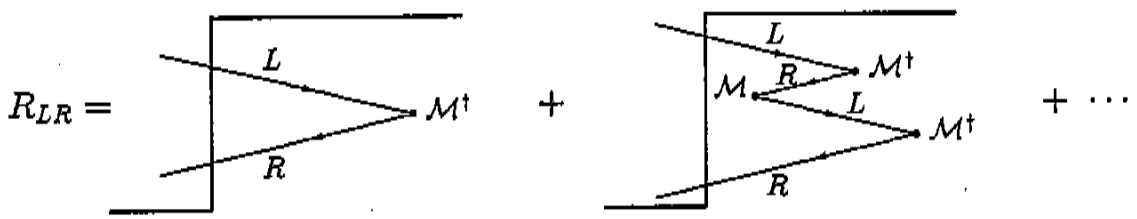
$R_{LR} =$
L
R
$\mathcal{M}^\dagger$
+
L
R
$\mathcal{M}$
$\mathcal{M}^\dagger$
L
R
$\mathcal{M}^\dagger$
+ ···

Fig. 4

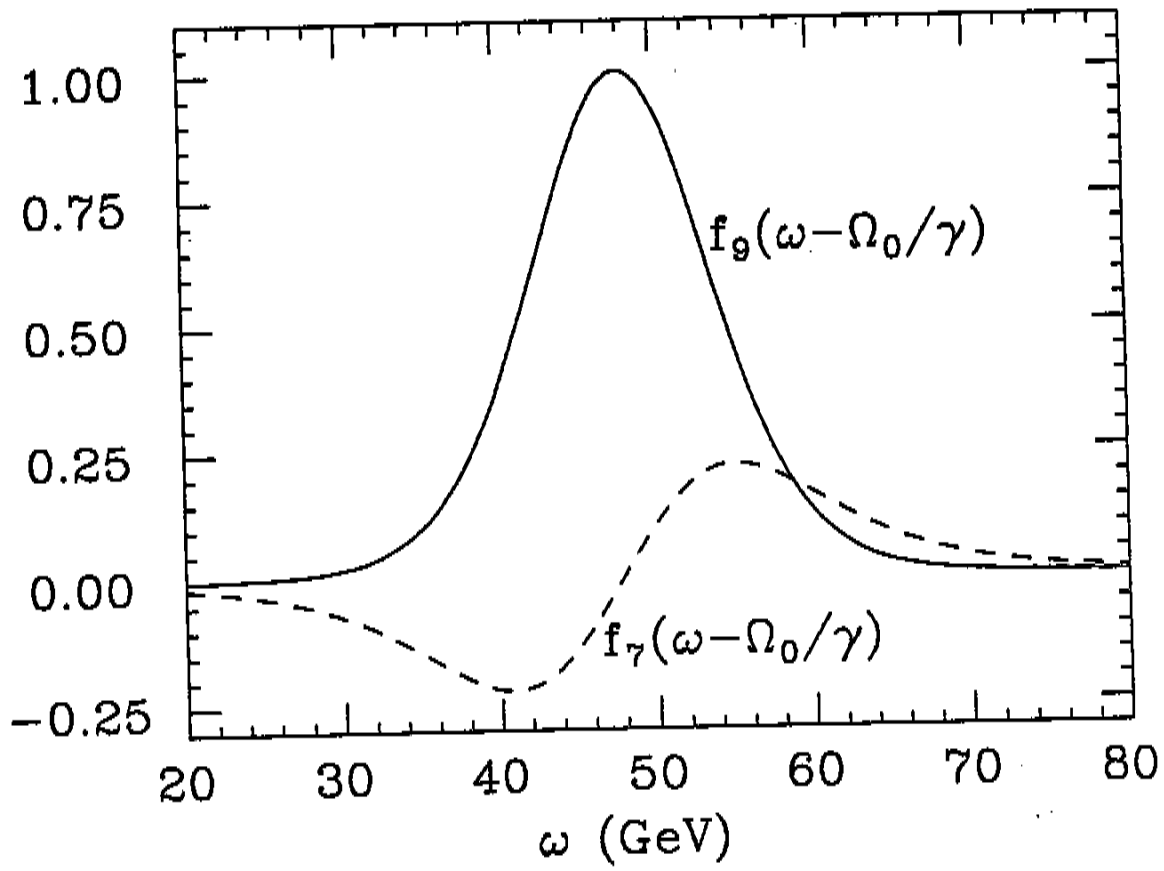
1.00
0.75
0.50
0.25
0.00
−0.25
20
30
40
50
60
70
80
ω (GeV)
$f_9(\omega-\Omega_0/\gamma)$
$f_7(\omega-\Omega_0/\gamma)$

Fig. 5

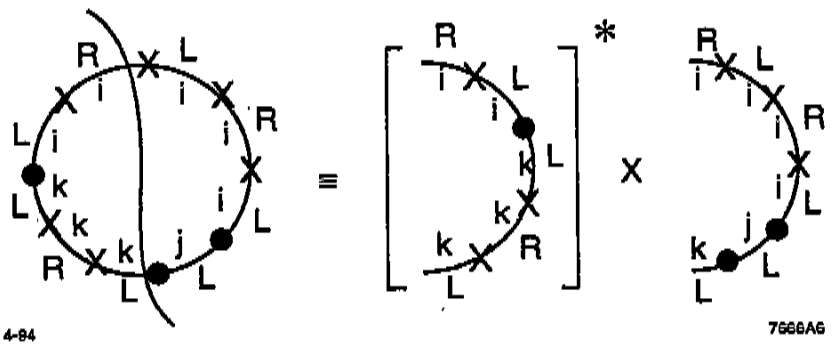
≡
X
4-84
7666A6

Fig. 6